DRDC-RDDC-2014-P16

(RTO) Characterization of the time-dependent behaviour of dielectric barrier discharge plasma actuators

Arash Naghib-Lahouti* and Rogerio Pimentel†
Defence R&D Canada, Valcartier, Québec, G3J 1X5, Canada

Philippe Lavoie‡
University of Toronto Institute for Aerospace Studies, Toronto, Ontario, M3H 5T6, Canada

Phase-locked PIV has been used to investigate the time-dependent behaviour of a Dielectric Barrier Discharge (DBD) plasma actuator, excited by a sine-wave signal with peak-to-peak amplitudes between 7.2 kV and 10 kV, and frequencies of 2.5 kHz and 4 kHz. The results indicate that the maximum induced velocity and body force occur during the negative half-cycle of the excitation signal, with a phase lag relative to the excitation signal that grows when excitation voltage or frequency is increased. A smaller, secondary peak is observed in the induced body force, occurring during the positive half-cycle of the excitation signal. The results suggest that this peak is due to formation of a secondary high-velocity region due to local discharges near the grounded electrode. Analysis of the induced body force, estimated using momentum balance in a control volume surrounding the actuator, indicates the significant role of the shear force acting on the actuator surface for the present configuration. The variability in the results of different methods for determining the shear force, and the difference observed in certain conditions between the estimated body forces and those measured directly using a balance highlight the need for further improving the methodology for body force prediction based on PIV measurements.

I. Introduction

DIELECTRIC barrier discharge plasma actuators are gaining increasing acceptance as flow control devices, due to their unique features including independence from external sources of flow, and relatively low geometric profile, which makes them relatively easy to implement. The growing range of successful applications of plasma actuators for flow control includes control of transition of a laminar boundary layer,[1,2] control of flow separation on an airfoil,[3] and control of bluff body wakes.[4] Many of these applications involve unsteady flow phenomena of various time scales, which require the use of active flow control for more effective interaction with the flow. One of the important aspects in active flow control is the time-dependent behaviour of the actuator, and in particular its temporal response to actuator commands. This characteristic becomes particularly significant when the dominant time scales of the flow phenomenon and the temporal response of the actuator are of the same order of magnitude. The study of the time-dependent behaviour of plasma actuators also provides a better understanding of their flow physics, which are closely related to the characteristics of the unsteady excitation signal. Improving the current knowledge in the two above-mentioned areas has been the primary motivation of the present study.

Various measurement techniques have been used in the past to investigate the time-dependent characteristics of the flow induced by plasma actuators. Boucinha *et al.*[5] have used Laser Doppler Velocimetry

*NSERC visiting research fellow, Defence R&D Canada, Valcartier, QC G3J 1X5, Canada.
†Defence scientist, Defence R&D Canada, Valcartier, QC G3J 1X5, Canada, AIAA member.
‡Associate Professor, University of Toronto Institute for Aerospace Studies, 4925 Dufferin St., Toronto, ON M3H 5T6, Canada, Senior AIAA member.

(LDV) to measure the induced velocity at a number of significant locations near a Dielectric Barrier Discharge (DBD) plasma actuator. In their experiments, the velocity generated by exciting the actuator at a frequency of 1 kHz was measured at an average sampling rate of 4 kHz. While this sampling rate made it possible to demonstrate that the flow induced by the actuator varied through the excitation cycle, it was not sufficient to produce a high-resolution time-resolved representation of the behaviour of the induced flow. Furthermore, since LDV is a line of sight technique, a large number of separate measurements would be needed to characterize the entire flow field using this technique, making this measurement method particularly susceptible to eventual deterioration of the plasma actuator in long-duration operation.[6]

Kotsonis and Ghaemi[7] have used high-speed Particle Image Velocimetry (PIV) to characterize the flow field around DBD plasma actuators excited by various waveforms. In their experiments, the actuator was excited at a frequency of 625 Hz, and the sampling rate was 6 kHz. While the time-dependent behaviour of the actuator was resolved with remarkable temporal resolution in their study, the excitation frequency was much lower than typical values found in most other studies. This highlights the fact that application of this technique in general is limited to lower actuator excitation frequencies, due to limits in the sampling frequency of current high-speed PIV systems and the prohibitive cost and technical challenges of very high frequency PIV measurements. As an example, to obtain a similar temporal resolution for a plasma actuator excited at a typical frequency of 5 kHz, a high-speed PIV system with an unusually high sampling rate of 50 kHz would be needed.

DBD plasma actuators are usually excited using an AC signal. The periodic nature of the excitation signal makes it possible to use it as a triggering source for synchronized, phase-locked measurements. Phase-locked PIV measurement is an accessible and consistent alternative to the above-mentioned time-resolved techniques for characterizing the time-dependent behaviour of flow induced by plasma actuators. One of the earliest examples of the use of this technique is the study by Kim *et al.*[8] to investigate the role of elevated levels of oxygen on improvement of the velocity induced during the positive half-cycle of the excitation voltage. This study shows the merit of this technique for measuring the entire flow field at the desired instances through the excitation cycle using a conventional low-speed PIV system, even when the excitation frequency is relatively large. Another example of the utilization of phase-locked PIV measurements to characterize the time-dependent behaviour of plasma actuators is the study by Murphy *et al.*,[9] in which the effect of the amplitude of the excitation voltage on spatial and temporal variations of peak momentum transfer throughout the excitation cycle have been investigated.

The present study extends the scope of the study by Murphy *et al.*,[9] while retaining the same physical configuration and geometry for the plasma actuator, to facilitate comparison with previous findings. The focus of the present study is to characterize the phase-dependent behaviour of the maximum induced velocity and its location, as well as the induced body force through the excitation cycle, using phase-locked PIV measurements with improved temporal resolution. Specifically, the number of phase intervals at which PIV measurements are carried out through the excitation cycle, is increased from 8 to 12, with concentration in the vicinity of the phase angles associated with the maximums of the induced velocity and body force. Furthermore, the measurements are carried out at two excitation frequencies, thus making it possible to investigate the effects of excitation frequency on the above-mentioned phase-dependent characteristics. Finally, a detailed investigation of the wall shear stress as a significant contributor to the induced body force is carried out in the present study. This investigation includes the effect of various estimation methods on the body force component resulting from wall shear stress, and an attempt to validate the body force estimation methods based on PIV measurements against direct body force measurements using a force balance.

II. Experimental setup

The plasma actuator used in the present experiments comprised of two 80 μm thick copper electrodes, separated by 4 layers of Kapton® tape as dielectric. Each layer of Kapton® tape was 0.089 mm thick, bringing the total dielectric thickness to 0.356 mm. A plate made of polymethyl methacrylate (PMMA) with a thickness of 3 mm was used as substrate, to support the electrodes and the dielectric layer. The widths of the exposed and grounded electrodes were 6.35 mm and 19.05 mm, respectively, and the span of both electrodes was 150 mm. No gap existed between the adjacent edges of the exposed and the grounded electrodes. The actuator was placed in a cubic chamber with a side length of 0.68 m, made of transparent PMMA, to isolate it from ambient disturbances.

The plasma actuator was excited by a sine-wave signal, which was generated by an Agilent 33210A

function generator, and amplified by a ratio of 2000:1 using a Trek Model 20/20C amplifier. The accuracy of the excitation signal was ±0.05 Hz at 2.5 kHz and ±0.08 Hz at 4.0 kHz. During each experiment, the electric power consumption of the plasma actuator was measured using the probe capacitance method described by Kriegseis *et al.*,[10] with the capacitance of the probe capacitor being three orders of magnitude larger than the cold capacitance of the plasma actuator. The excitation voltage of the plasma actuator and the voltage across the probe capacitor were measured and recorded using a Rigol 1052E digital oscilloscope, simultaneous with the PIV over a period of 20 ms, which spanned 50 and 80 cycles at the excitation frequencies of 2.5 kHz and 4.0 kHz, respectively. The electric current was estimated based on the time derivative of the electric charge accumulated across the probe capacitor. A schematic diagram of the electronic components of the plasma actuator setup is shown in Figure 1.

PIV technique was used to measure the velocity field around the actuator. A LaVision PIV system including an Imager SX-4M CCD camera with a resolution of 2386 × 1776 pixels equipped with a Sigma 105 mm f/2.8 macro lens, and an Evergreen 200 mJ/pulse Nd-YAG laser was utilized. Measurements were carried out in a domain measuring 31.5 mm in the horizontal (x) direction and 15 mm in the wall-normal (y) direction, with the downstream edge of the exposed electrode ($x = y = 0$) located 8 mm upstream of the centre of the measurement domain. Velocity vector fields were obtained using a cross-correlation scheme in 1616 interrogations windows with 50% overlap, resulting an array of 295 × 222 vectors with a spatial resolution (spacing between adjacent vectors) of 0.107 mm. Phase-locked measurements were carried out using the excitation signal generated by the function generator as an external trigger for the PIV system Programmable Timing Unit (PTU). The phase angle for each set of measurements was specified by adjusting the time delay between the trigger signal and the recording of the image pairs in the PIV system. For each experiment involving a particular combination of excitation parameters, phase-locked measurements were carried out at 12 phase angles at $\pi/4$ rad intervals in the positive half-cycle of the excitation signal, and $\pi/8$ rad intervals in the negative half-cycle, with 300 image pairs for each phase angle.

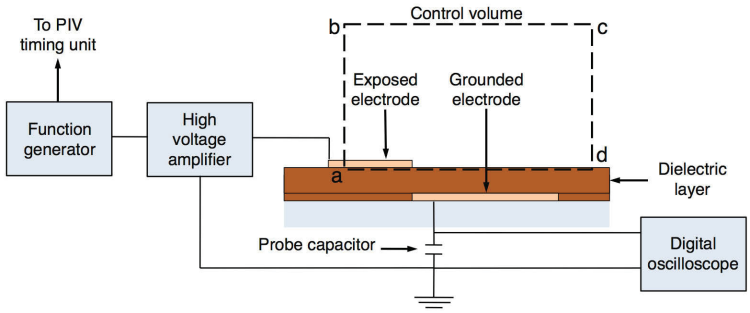

Figure 1. Schematic view of the plasma actuator setup showing the position of the control volume for body force estimation relative to the actuator.

Direct measurements of the force generated by the plasma actuator was carried out using a Ohaus Explorer EX324 balance, which had a resolution of 0.0001 g. During the force measurement experiments, the excitation signal was generated using a National Instruments PXI-5402 arbitrary function generator and amplified using a Matsusada AMP-20P20 amplifier. The balance was placed in a grounded Faraday cage, to minimize electromagnetic interference, and the actuator was placed on the balance vertically with the grounded electrode above the exposed electrode, using a rigid mechanical support. Electrical connection between the actuator and the power supply was established using bead chains, to ensure that the connection does not restrict the actuator during force measurements.

III. Velocity field

An example of the results of phase-locked PIV measurements of the velocity field around the plasma actuator is shown in Figure 2. The figure shows the evolution of the induced velocity magnitude ($|V| = \sqrt{u^2 + v^2}$) throughout the excitation cycle, for an excitation voltage of 8.8 kV_{pp} and an excitation frequency of 4 kHz. It can be observed that a phase lag exists between the maximum of the excitation voltage, which occurs at $\Phi = 0$, and the maximum of the induced velocity, which occurs at at $\Phi = 11\pi/8$. The maximum of the induced velocity occurs during the negative half-cycle of the excitation voltage, when the exposed electrode has a negative charge. The phase lag, which is of particular interest in application of plasma actuators for active flow control, can be investigated in more detail by examining the time-dependent behaviour of the maximum induced velocity relative to the excitation signal, for various combinations of excitation parameters.

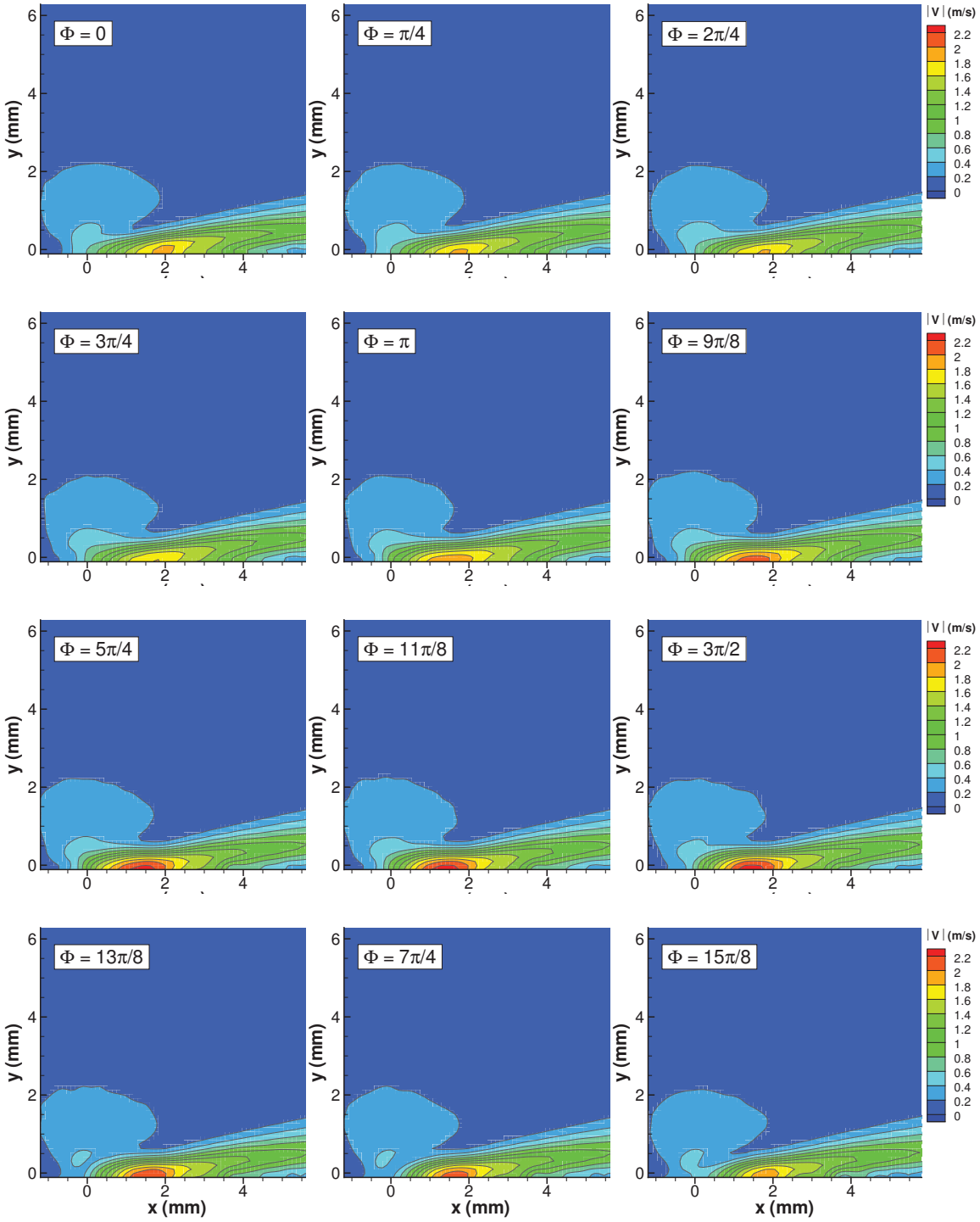

Figure 2. Phase-averaged contours of the induced velocity magnitude $|V| = \sqrt{u^2 + v^2}$ for an excitation voltage of 8.8 kV_{pp} and excitation frequency of 4 kHz.

Figure 3 shows the variation of maximum magnitude of the induced velocity throughout the excitation cycle for three excitation voltages of 7.2 kV_{pp}, 8.8 kV_{pp}, and 10.0 kV_{pp}, applied at 2.5 kHz (Figure 3a) and 4.0 kHz (Figure 3b). The average values of the induced velocity magnitude are in close agreement with those reported by Murphy *et al.*[11] for the same plasma actuator. However, the figure indicates that the phase lag between the maximum induced velocity and the excitation voltage is not constant. Figure 4 shows the trend of variation of the phase lag with excitation parameters. It can be observed that the phase lag increases slightly when the actuator is excited with a higher voltage. This effect is more pronounced at the excitation frequency of 4 kHz, where relatively larger values of phase lag are observed.

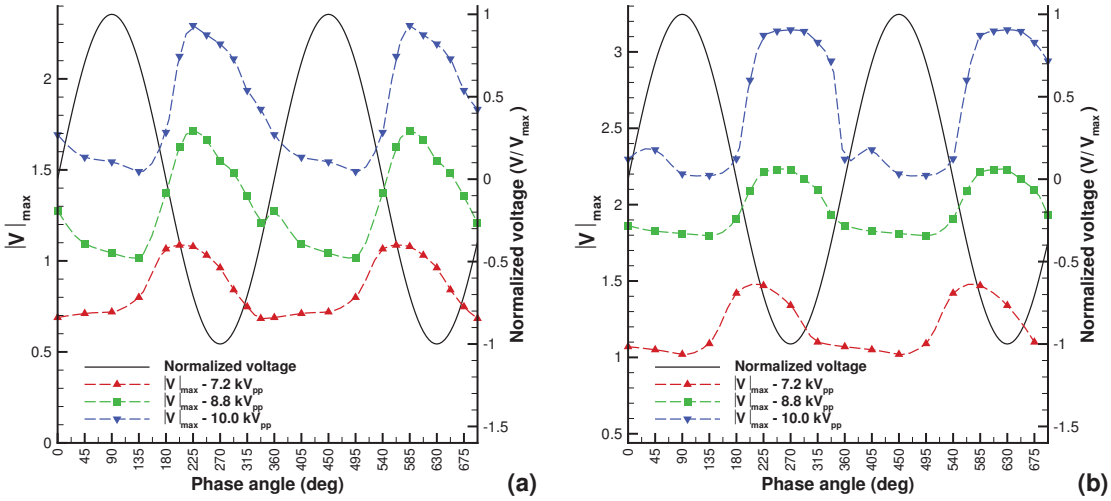

Figure 3. Phase-averaged values of the maximum magnitude of the induced velocity $|V|_{max}$ for three excitation voltages applied at (a) 2.5 kHz and (b) 4 kHz.

Another interesting aspect of the time dependent behaviour of the plasma actuator is the location of the maximum induced velocity within the measurement domain. As shown in Figure 5, the location of maximum velocity depends on the phase angle, with a general trend in which the location of the maximum induced velocity is closer to the downstream edge of the exposed electrode ($x = y = 0$) during the negative half-cycle of the excitation signal, and farther from it during the positive half cycle. This trend, which is the opposite of the phase-dependent behaviour of the maximum induced velocity (Figure 3) suggests that during the negative-half cycle, when the exposed electrode has a negative charge, the largest velocity in the domain is induced by the exposed electrode. Conversely, during the positive half-cycle of the excitation voltage, the largest velocity is induced by the grounded electrode, which has a negative charge. The velocity induced by the grounded electrode is smaller than that induced by the exposed electrode, because the grounded electrode is isolated from the fluid by the dielectric layer.

IV. The body force

The results of the phase-locked measurements of the velocity field around the plasma actuator can be used to estimate the body force generated by the actuator, based on the balance of momentum in a control volume surrounding the actuator (Figure 1). This method, which has been developed by Versailles *et al.*,[12] assumes a steady, incompressible flow with constant and uniform pressure on the boundaries of the control volume. The formulation for this method can be summarized by the following equation

$$f = \rho \int_{ab} u^2 \mathrm{d}y + \rho \int_{bc} uv \mathrm{d}x - \rho \int_{cd} u^2 \mathrm{d}y + \int_{ad} \mu \left(\frac{\mathrm{d}u}{\mathrm{d}y}\right)_{\text{wall}} \mathrm{d}x. \quad (1)$$

In Eq (1), f is the body force generated by the actuator in the horizontal (x) direction. The last term in Eq (1) represents the shear force generated on the wall (along the boundary ad in Figure 1). The effect of the location of the boundaries on the estimated body force has been investigated in the study by Murphy *et al.*[11] In accordance with the findings reported in their study, which involves an actuator with the same

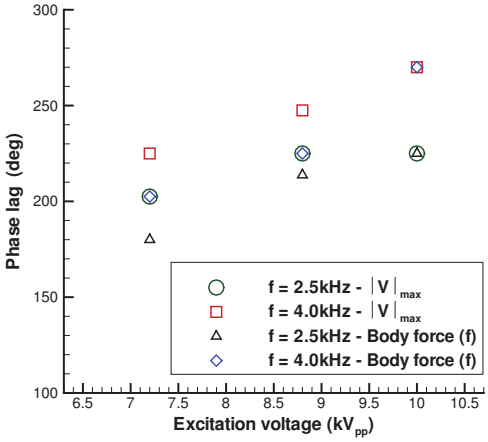

Figure 4. Phase lag between the maxima of the induced velocity magnitude ($|V|$) and body force (f), and the excitation voltage.

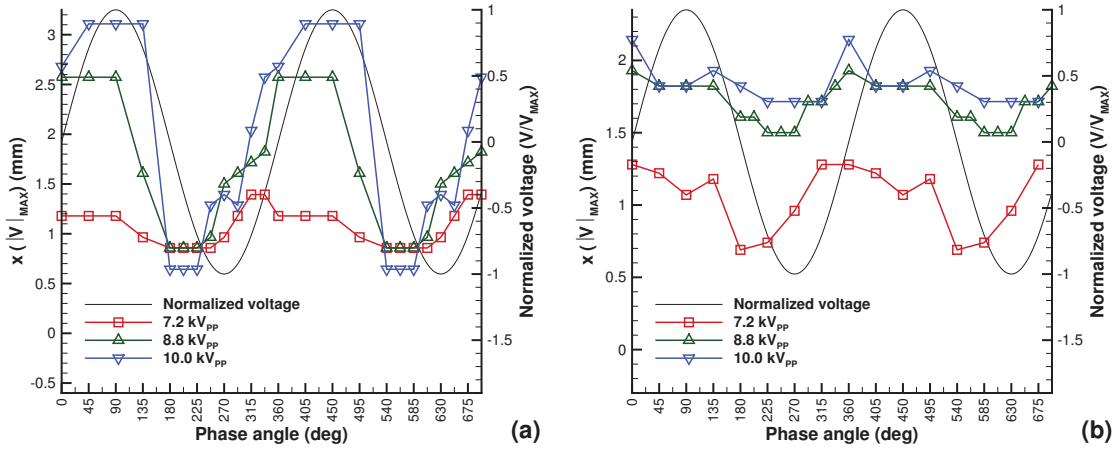

Figure 5. Phase-dependent variations of the location of the maximum magnitude of the induced velocity $x(|V|_{max})$ for three excitation voltages applied at (a) 2.5 kHz and (b) 4 kHz.

geometry and dimensions, the boundaries ab and cd have been placed at $x = -2$ mm and $x = 15$ mm, respectively, and the boundary bc has been placed at $y = 15$ mm for the present calculations.

Figure 6 show the phase-dependent behaviour of the estimated body force for three excitation voltages (7.2 kV_{pp}, 8.8 kV_{pp}, and 10.0 kV_{pp}), applied at excitation frequencies of 2.5 kHz and 4.0 kHz. The behaviour of the body force is generally similar to that of the induced velocity, as discussed in Section III. The primary peak in the body force corresponds to the maximum induced velocity, as they both appear at the same phase angle during the negative half-cycle of the excitation signal. Similarly, a phase lag exists between the maximum body force and the peak excitation voltage, which increases slightly when the actuator is excited with a higher voltage, as shown in Figure 4. This effect is more pronounced at the excitation frequency of 4 kHz, where relatively larger values of phase lag are observed.

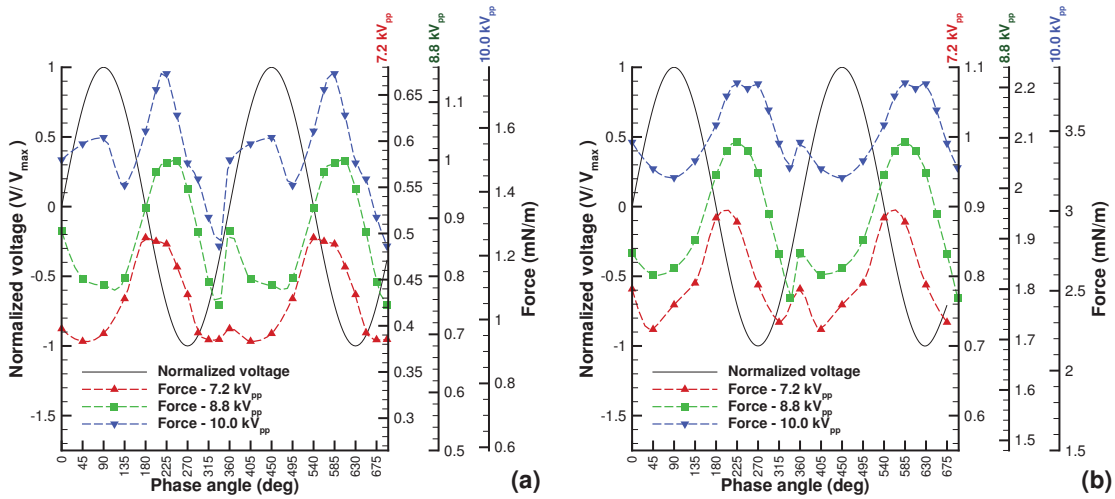

Figure 6. Phase-averaged values of the induced body force for three excitation voltages applied at (a) 2.5 kHz and (b) 4.0 KHz.

Figure 6 also shows a smaller secondary peak in the phase-dependent variations of the body force, at the approximate phase angle of $\Phi = 2\pi$. An investigation of the time-dependent variation of the electric current passing through the plasma actuator, shown in Figure 7 for an excitation voltage of 8.8 kV_{pp} and frequency of 4.0 kHz, indicates that the phase angle of this secondary peak corresponds with spikes in the positive electric current, which are believed to be caused small and localized discharges associated with formation of the plasma near the grounded electrode during the positive half cycle of the excitation signal.[7] The phase-dependent behaviour of the location of the maximum induced velocity magnitude (Figure 5) supports this hypothesis, because it shows that during the positive half of the excitation signal, the location of the maximum induced velocity shifts downstream towards the grounded electrode. Kotsonis and Ghaemi[7] have reported a similar correspondence between the spikes in the positive electric current and a secondary peak in the local fluid acceleration induced by the plasma actuator through the positive half cycle of the excitation signal, based on time-resolve PIV measurements of the velocity field. While the observation by Kotsonis and Ghaemi[7] is limited to a single point in the flow field, the results of the present study indicate that the effects of the formation of plasma near the grounded electrode during the positive half cycle of the excitation signal is more widespread, as indicated by the secondary peak in the body force.

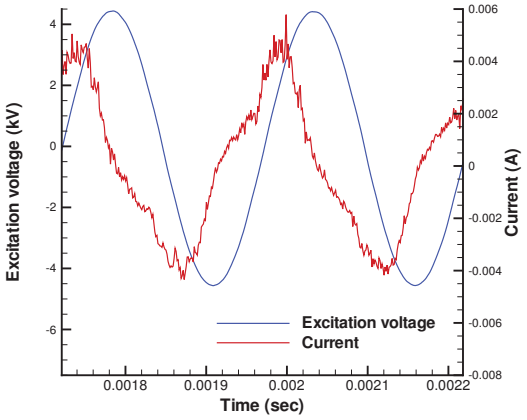

Figure 7. A sample of the time series of the excitation voltage and current from the experiment at 8.8 kV_{pp} and 4.0 KHz, showing the current spikes.

The ratio of the magnitude of the secondary peak of the body force (f_2) to the primary peak (f_1) is shown in Figure 8. The figure indicates that the relative magnitude of the secondary peak grows as excitation voltage and frequency increase. Considering the fact that the secondary peak is associated with the formation of plasma over the grounded electrode during the positive half cycle of the excitation signal, this behaviour indicates that the effectiveness of the dielectric layer in isolating the grounded electrode from the fluid decreases at higher excitation voltages and frequencies.

Murphy *et al.*[11] have shown that the wall shear stress, represented by the last term in Eq (2), constitutes up to 30% of the body force. Considering the significance of this term, the role of the estimation method for the wall-normal derivative $\left(\frac{\mathrm{d}u}{\mathrm{d}y}\right)_{\mathrm{wall}}$ in the shear stress term has been addressed in the present study. In previous studies[11,9] this term has been estimated using the following first order numerical derivation scheme

$$\left(\frac{\mathrm{d}u}{\mathrm{d}y}\right)_{\mathrm{wall}} = \frac{u_1}{\Delta y}, \tag{2}$$

in which u_1 is the horizontal velocity component at the first measurement point above the boundary ad, and Δy is the distance of the measurement point from the boundary. This method is evidently dependent on the spatial resolution of the measurement technique in the wall-normal direction, as well as the accuracy of the velocity measured adjacent to the wall, which is usually affected by reflections from the wall and reduced particle density in PIV measurements. The other approach for estimating the wall normal derivative is based on the assumption that the plasma actuator generates a two-dimensional laminar wall jet. This assumption has been validated by Murphy *et al.*[11] for the present plasma actuator configuration. Glauert[13] has shown that the self-similar velocity profile in a two-dimensional wall jet $f'(\eta)$ is given by the solution of the following ordinary differential equation

$$f''' + ff'' + 2f' = 0, \tag{3}$$

with boundary conditions $f(0) = f'(0) = 0$ and $f'(\infty) = 0$. The term $\left(\frac{\mathrm{d}u}{\mathrm{d}y}\right)_{\mathrm{wall}}$ is then estimated by scaling the derivative of the self-similar velocity profile, using

$$\left(\frac{\mathrm{d}u}{\mathrm{d}y}\right)_{\mathrm{wall}} = \left(\frac{u_{max}}{f'_{max}}\right)\left(\frac{\eta_{max}}{y_{max}}\right)\left(\frac{\mathrm{d}f'}{\mathrm{d}\eta}\right)_{\mathrm{wall}}, \tag{4}$$

in which u_{max} is the local maximum velocity of the wall jet at any given streamwise (x) location, and y_{max} is the location of the maximum velocity in the wall-normal direction. Numerical solution of Eq.3 yields the values of the terms in Eq.4, as $\left(\frac{\mathrm{d}f'}{\mathrm{d}\eta}\right)_{\mathrm{wall}} = 0.2222$, $f'_{max} = 0.3150$, and $\eta_{max} = 2.0287$. Substitution of these values simplifies Eq.4 to

$$\left(\frac{\mathrm{d}u}{\mathrm{d}y}\right)_{\mathrm{wall}} = 1.4310\frac{u_{max}}{y_{max}}. \tag{5}$$

Rather than relying on the velocity adjacent to the wall, this method relies on the maximum velocity of the wall jet, which usually occurs away from the wall. Therefore, it is less sensitive to spatial resolution of the PIV measurements and less likely to be affected by the quality of velocity measurement adjacent to the wall.

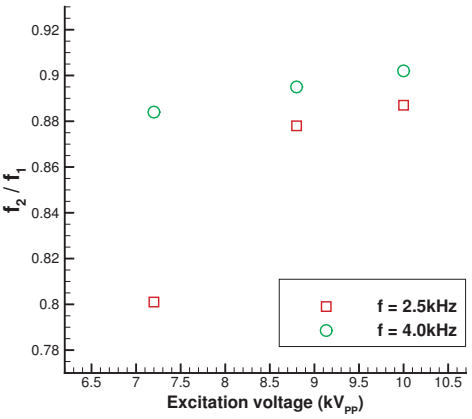

Figure 8. The ratio of the magnitude of the secondary peak (f_2) of the body force to the primary peak (f_1).

The results of estimation of the body force using the two above-mentioned methods to estimate the wall-normal derivative in the shear stress term are compared in Figure 9 for excitation voltages of 8.8 kV_{pp} and 10.0 kV_{pp}, applied at $f = 2.5$ kHz. The figures that a difference of up to 25% exists between the values of the body force obtained using the two methods. The body force obtained using the wall jet method (Eq.5) for estimating the wall shear stress term, is consistently larger than that obtained using the first order numerical estimation (Eq.2).

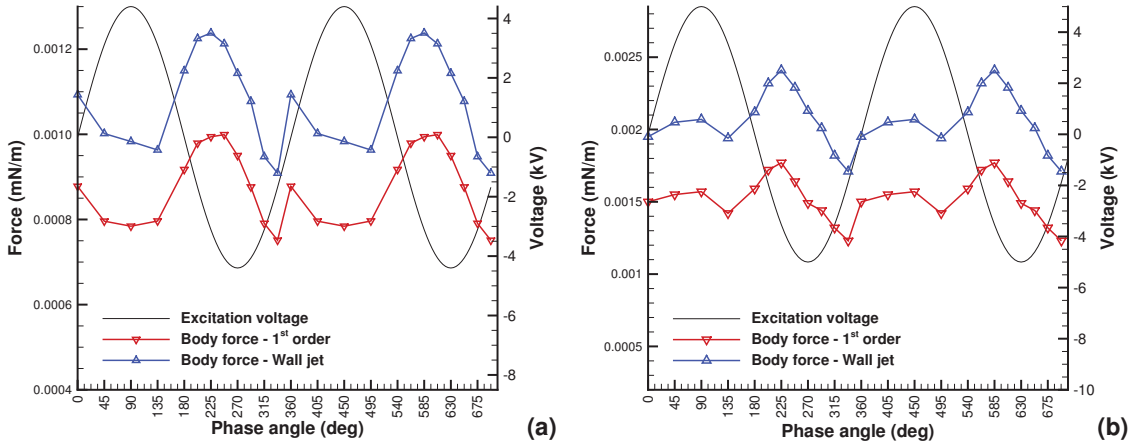

Figure 9. Comparison of the body forces obtained using the 1st order numerical estimation and the wall jet model for determining the wall shear stress term, for excitation voltages of (a) 8.8 kV$_{pp}$ and (b) 10.0 kV$_{pp}$, applied at f=2.5 kHz.

In order to evaluate the results of the estimation of the body force based on PIV measurements, direct measurements of the force generated by the actuator were carried out, as described in Section II. For certain plasma actuator configurations, for example those studied by by Hoskinson *et al.*,[14] the shear force acting on the surface due to the flow induced by the actuator is small compared to the force resulting from the induced momentum. Therefore, the force measured by the balance is close to the momentum component of the force generated by the actuator, represented by the first 3 terms of Eq.1. However, the results of the present study and the study by Murphy *et al.*[11] indicate that for the present plasma actuator configuration, the shear force comprises a significant part of the actuator body force and is not negligible. Therefore, the force measured directly by the balance is expected to include the effect of the shear force, by the last term in Eq.1, in accordance with the findings of Ashpis and Laun.[15]

The results of the direct force measurements are compared to the forces obtained based on the PIV measurements in Figure 10. It can be observed that in all combinations of excitation voltage and frequency, the results of the direct force measurements are larger than the momentum-based component of the force estimated using the first 3 terms of Eq.1, and that at the excitation frequency of f = 2.5 kHz, they are close to the estimated total force, which includes the shear force component. This observation confirms that the shear force component is indeed a significant contributor to the total body force in the present plasma actuator configuration. The difference between the results of direct force measurements and the estimated total force, however, suggests that further improvement in the methodology for estimating the shear force component may be needed.

V. Conclusion

In the present study, phase-locked PIV measurements have been carried out using a conventional PIV system, to investigate the time-dependent behaviour of plasma actuators with a temporal resolution comparable to those achieved using high-repetition-rate PIV in previous studies. The phase-locked measurement technique has been found to be advantageous over TR-PIV, because it allows measurement of the time-dependent behaviour at relatively high excitation frequencies (up to 4 KHz in the present experiments), without requiring a high-speed cameras and laser light source. Measurements have been carried out in 12 phase intervals throughout the excitation signal applied at 4 kHz. To achieve a similar temporal resolution, a TR-PIV system would require a sampling frequency up to 96 kHz, which is beyond the capability of most commercially available systems. The present technique can also provide results with more adequate spatial resolution as does not suffer from decreased camera resolution associated with cameras operated at high capture rates. Using the full resolution of the PIV camera, a vector spacing of 0.1 mm has been achieved in

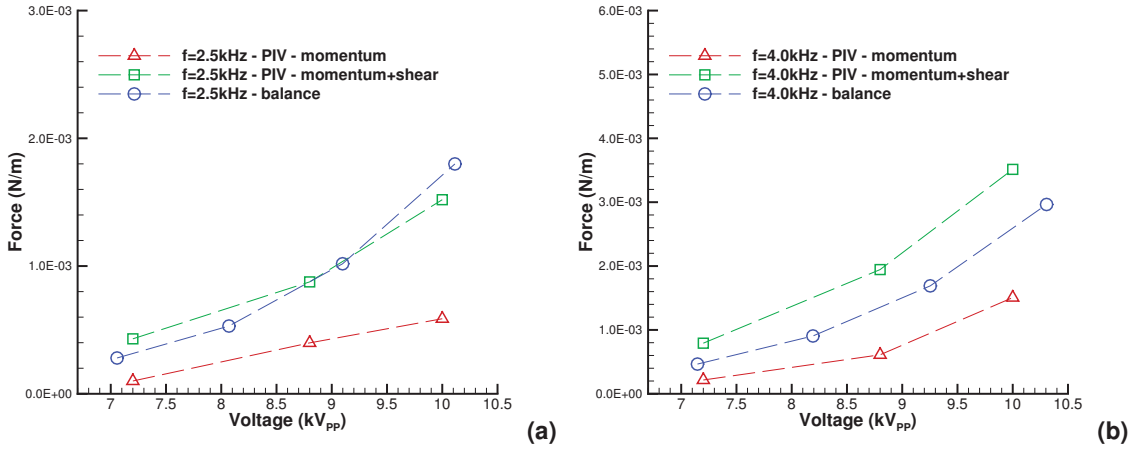

Figure 10. Comparison of the results of the direct force measurements with the forces obtained based on PIV measurements using the control volume method, at (a) f=2.5 kHz and (b) f=4 kHz.

the present experiments in a 31.5 mm-wide domain.

The results indicate that a phase lag exists between the maximum induced velocity by the plasma actuator and the excitation signal. A similar phase lag also exists between the induced body force and the excitation signal. The phase lag varies between 180° and 270°, depending on the excitation voltage and frequency. In general, the phase lag increases when the excitation voltage or frequency are increased. This finding is significant for application of plasma actuators in active flow control, especially when the characteristic time scales of the flow phenomena are close to those of the actuator.

The phase-dependent behaviour of the body force, estimated using a control volume method based on the results of the PIV measurements, shows that the maximum induced body force throughout the excitation cycle is concurrent with the negative half-cycle of the excitation signal. A secondary peak has also been found to occur during the positive half-cycle of the excitation signal. The magnitude of the secondary peak, which varies between 80% and 90% of the maximum induced body force, increases when the excitation voltage or frequency is increased. The present results indicate that the secondary peak is due to the formation of a secondary high-velocity region near the grounded electrode during the positive half-cycle of the excitation signal. The formation of this secondary high-velocity region has been observed in the TR-PIV measurements conducted by Kotsonis and Ghaemi,[7] and attributed to small and localized discharges associated with formation of the plasma near the grounded electrode. The spikes of the electric current observed in the present experiments during the positive half-cycle of the excitation signal support this hypothesis. The trend of variation of the magnitude of secondary peak indicates that the effectiveness of the dielectric layer in isolating the grounded electrode from the fluid decreases at higher excitation voltages and frequencies.

For the present plasma actuator configuration, the shear force acting on the surface of the actuator, which is proportional to the wall-normal derivative of the streamwise velocity at the surface, is a significant contributor to the total body force estimated using the control volume method. Two different methods have been utilized to determine the wall normal derivative, resulting in up to 25% variation in the estimated body force. In order to evaluate the control volume method for estimating the body force based on PIV results, direct force balance measurements have been carried out. Comparison of the results shows that at the excitation frequency of $f = 2.5$ kHz, the PIV-based body forces are close to those obtained from direct balance measurements. At $f = 4$ kHz, however, the control volume method over-estimates the body force, indicating that further improvement in the method, and in particular the estimation of the shear force is required.

Acknowledgement

The authors would like to acknowledge the financial support of the National Science and Engineering Research Council of Canada (NSERC) and DND TIF project 01gy01.

References

[1]Grundmann, S. and Tropea, C., "Active cancellation of artificially introduced Tollmien-Schlichting waves using plasma actuators," *Experiments in Fluids*, Vol. 44, 2008, pp. 795–806.

[2]Hanson, R., Lavoie, P., Naguib, A., and Morrison, J., "Transient growth instability cancellation by a plasma actuator array," *Experiments in Fluids*, Vol. 49, 2010, pp. 1339–1348.

[3]Jukes, T., Segawa, T., and Furutani, H., "Active flow separation control on a NACA 4418 airfoil using DBD vortex generators and FBG sensors," *50th AIAA aerospace sciences meeting*, No. AIAA 2012-1193, Nashville, Tennessee, USA, 2012.

[4]Kozlov, Z. and Thomas, F., "Bluff-body flow control via two types of dielectric barrier discharge plasma actuation," *AIAA Journal*, Vol. 49, No. 9, 2011, pp. 1919–1931.

[5]Boucinha, V., Joussot, R., Magnier, P., Weber, R., and Leroy-Chesneau, A., "Characterization of the ionic wind produced by a DBD actuator designed to control the laminar-to-turbulent transition," *Proceedings of the 14th International Symp. on Application of Laser Techniques to Fluid Mechanics*, No. 1352, Lisbon, Portugal, 2008.

[6]Hanson, R., Houser, N., and Lavoie, P., "Dielectric material degradation monitoring of dielectric barrier discharge plasma actuators," *Journal of Applied Physics*, Vol. 115, No. 043301, 2014.

[7]Kotsonis, M. and Ghaemi, S., "Performance improvement of plasma actuators using asymmetric high voltage waveforms," *Journal of Physics D: Applied Physics*, Vol. 45, No. 4, 2012, pp. 045204.

[8]Kim, W., Do, H., Mungal, M. G., and Cappelli, M. A., "On the role of oxygen in dielectric barrier discharge actuation of aerodynamic flows," *Applied Physics Letters*, Vol. 91, 2007, pp. 181501–1–3.

[9]Murphy, J., Kriegseis, J., and Lavoie, P., "Scaling of maximum velocity, body force, and power consumption of dielectric barrier discharge plasma actuators via particle image velocimetry," *Journal of Applied Physics*, Vol. 113, 2013, pp. 243301–1–10.

[10]Kriegseis, J., Moller, B., Grundmann, S., and Tropea, C., "Capacitance and power consumption quantification of Dielectric Barrier Discharge (DBD) plasma actuators," *Journal of Electrostatics*, Vol. 69, 2011, pp. 302–312.

[11]Murphy, J. and Lavoie, P., "Characterization of DBD plasma actuators via PIV measurements," *51st AIAA Aerospace Sciences Meeting*, No. AIAA 2013-0346, Grapevine, Texas, USA, 2013.

[12]Versailles, P., Gingras-Gosselin, V., and Vo, H. D., "Impact of pressure and temperature on the performance of plasma actuators," *AIAA Journal*, Vol. 48, 2010, pp. 859–863.

[13]Glauert, M. B., "The wall jet," *Journal of Fluid Mechanics*, Vol. 1, No. 6, 1956, pp. 625–643.

[14]Hoskinson, R., Hershkowitz, N., and Ashpis, D., "Force measurements of single and double barrier DBD plasma actuators in quiescent air," *Journal of Physics D: Applied Physics*, Vol. 41, No. 24, 2008, pp. 245209–1–10.

[15]Ashpis, D. and Laun, M., "Dielectric Barrier Discharge (DBD) plasma actuator thrust measurement methodology incorporating new anti-thrust hypothesis," *52st AIAA Aerospace Sciences Meeting*, No. AIAA 2013-0486, National Harbor, Maryland, USA, 2014.